VARIABILITY OF AEROSOL OPTICAL PROPERTIES OVER HEFEI DURING SEPTEMBER 1993 TO SEPTEMBER 1994

Zhou Jun (周军), *Wang Zhi'en* (王志恩), *Han Jiecai* (韩接才), *Hu Huanling* (胡欢陵)

Anhui Institute of Optics and Fine Mechanics, Chinese Academy of Sciences, Hefei 230031

and *Li Guojie* (李国杰)

Anhui Institute of Meteorological Sciences, Hefei 230061

Received March 11, 1995; revised July 21, 1995

ABSTRACT

An 8-wavelength sun-photometer has been operated at Hefei (31.31°N, 117.17°E) to monitor optical properties of atmospheric aerosols. Altogether 133 solar spectral extinction data were obtained on clear days during the period from September 1993 through September 1994. In this paper, the feature of the sun-photometer is briefly described. A relative aureole method is introduced, which can be used to monitor temporal evolution of aerosol loading during the sun-photometer calibration period. Temporal variabilities of spectral aerosol optical depths and Angstrom turbidity parameters are presented. Relation of these variabilities with synoptic and local meteorological conditions are analyzed and discussed. From measured spectral aerosol optical depths under some representative atmospheric conditions, columnar aerosol size distributions have been retrieved by a linearly constrained inversion method. These typical columnar aerosol size distributions are also presented and discussed.

Key words: aerosol, solar radiometry, optical depth, turbidity

I. INTRODUCTION

Atmospheric aerosol particles absorb and scatter both the incoming solar radiation and the emitted infrared energy from the earth. They are also involved in forming processes of cloud, fog and haze. Therefore, aerosol particles produce a very significant effect on the radiation budget in the earth-atmosphere system. Actually, they have been considered as one of key factors in the radiative transfer, climatic and environmental studies (Tanre et al. 1988).

Aerosol optical depth is a very important aerosol optical parameter characterizing the feature of aerosol particle extinction in vertical atmospheric column. From the wavelength dependence of aerosol optical depths, Angstrom turbidity parameters, i. e., Angstrom turbidity coefficient and wavelength exponent, can be evaluated. They provide a basis for estimating both quantity and predominant size distribution of aerosol particles in the atmosphere.

As aerosol optical depth and Angstrom turbidity parameters are highly variable both temporally and spatially, long-term measurements of these aerosol optical parameters at different representative places are of basic importance for studying radiative transfer, climate and environment. It is quite evident that the radiation budget affected by aerosol

particles can not be accurately determined without the sufficient information on these aerosol optical parameters and their temporal and spatial distributions.

In early 1960s the U. S. Environmental Protection Agency (EPA) and the National Oceanic and Atmospheric Administration (NOAA) supported a national network program to provide data on the geographical, seasonal and long-term variation of aerosol optical depths (Flowers et al. 1969). The results show very clearly the large differences in the aerosol optical depths which occur as a function of time of year and locality. Therefore, in recent decades, a great deal of effort in the form of observational studies has been devoted to determining the temporal and spatial variation of the aerosol optical parameters, such as spectral optical depths, Angstrom turbidity parameters, size distributions and refractive index (d'Almeida 1983; Flowers et al. 1969; King et al. 1980; Liu et al. 1990; Mohamed et al. 1986; Peterson et al. 1981; Pink et al. 1994).

In China, considerable progress has also been made in both observational and theoretical studies of the aerosol optical properties in recent years (Li et al. 1990; Mao et al. 1985; Qiu et al. 1986; 1988; Zhou et al. 1987). However, there still has been a lack of long-term or even middle-term studies that can provide information on the aerosol optical properties if determination of radiation budget affected by the aerosol is to be attempted. Therefore, long-term studies of aerosol optical properties are certainly required.

The objective of this study is to present the analysis results on the variability of the aerosol optical properties from September 1993 through September 1994. The data involve 133 clear day sun-photometer measurements in all. The measurement site is located at Anhui Institute of Optics and Fine Mechanics, 15 km west of Hefei (31.31°N, 117.17°E).

In this paper, the feature of the sun-photometer is briefly described. Results of relative aureole observations are presented, which provide information on temporal evolution of aerosol loading during the Langley calibration experiments. Then, temporal characteristics of spectral aerosol optical depths, Angstrom turbidity parameters and their relation with synoptic and local meteorological conditions are analyzed and discussed. From measured spectral aerosol optical depths under some representative atmospheric conditions, columnar aerosol size distributions have been retrieved by a linearly constrained inversion method. These typical columnar aerosol size distributions are also presented and discussed.

II. DTF-1 SUN-PHOTOMETER

A detailed explanation of the DTF-1 sun-photometer used in the presented study can be found in Zhou et al. (1994). Only a brief description is given here. The sun-photometer mainly consists of a sun-tracking unit, a detective unit and a computer, with a field of view 1°. The instrument has eight filters centered at 0.40, 0.44, 0.52, 0.612, 0.67, 0.78, 0.88 and 1.03 μm, with all halfwidths about 60 Å, but 100 Å for 1.03 μm. An EGG HUV-1100BQ amplifier/photodiode is used as detector. A thermostating box containing the detector ensures an internal temperature of 40°C with 1°C accuracy. Besides the solar spectral extinction observation, the sun-photometer can also take aureole measurements for each wavelength. Ten scattering angles are sampled between 2° and 30° from the sun direction. A variable gain amplifier of 12 decades (4096) and a 12-bit A/D converter

are used to meet such a large dynamic range. The solar spectral extinction measurement is made at 4-min intervals and aureole measurement at 30-min intervals. Both measurements are automatically controlled by an IBM-PC computer. All the measured data are recorded on a floppy disk for late processing. Examining instrumental parameters shows that measurement accuracy is better than 1%.

III. LANGLEY PLOTS CALIBRATION

The sun-photometer was calibrated at Mt. Huangshan weather station (30. 13°N, 118. 15°E, 1865 m asl) during the period of November 15 through 25, 1993 by using Langley method based on the Lamber-Beer equation (Herman et al. 1981):

$$V(\lambda, t) = RV_0(\lambda)\exp\{-\tau(\lambda)m(t)\}, \quad (1)$$

where $V(\lambda, t)$ is the output voltage of the sun-photometer on the ground level; $V_0(\lambda)$ the corresponding value at the top of atmosphere when it is at the mean sun-earth distance, i. e., the calibration value; R the correction factor for the sun-earth distance at the observation time; $\tau(\lambda)$ the atmospheric optical depth; $m(t)$ the atmospheric optical mass (relative) at the observation time; λ wavelength; and t the Beijing Time.

It is well known, the Langley method is based on the assumption that both atmospheric optical depth and sun-photometer's sensitivity remain constant during the period when measurements of $V(\lambda, t)$ are taken at different solar zeniths. If this assumption is true, the data-points giving the logarithms of $V(\lambda, t)$ plotted as a function of the atmospheric optical air mass $m(t)$ are found to form a straight line having an intercept of $\ln(V_0(\lambda))$ and a slop equal to $-\tau(\lambda)$. Therefore, for Langley method, both atmospheric stability and sun-photometer's constant sensitivity are absolutely required. The latter command is ensured by 1% measurement accuracy of the sun-photometer. Concerning the atmospheric stability, fluctuations in the atmospheric optical depth are closely related to the evolving feature of aerosol loading within the mixed layer. Thus, a clean and high altitude mountain is the site suitable for Langley calibration measurement. However, even at such a place, the atmospheric optical depth sometimes changes in time as a consequence of diurnal fluctuations of the aerosol concentration. On the other hand, Russell and Shaw (1975) have demonstrated that in cases where the atmospheric optical depth variation is linear with $1/m(t)$, the Langley plots give no indication of any system error. Therefore, an independent monitoring of temporal evolution of aerosol optical depth is needed. This can be done by aureole measurements taking simultaneously with the solar spectral extinction measurements. This method involves the temporal monitoring of the dimensionless ratio $\mu(\theta, \lambda, t)$ (relative aureole) given by (O'Neill et al. 1984):

$$\mu(\theta, \lambda, t) = \frac{I(\theta, \lambda, t)}{m(t)V(\lambda, t)} = \frac{\tau_a(\lambda, t)P(\cos\theta)}{4\pi}, \quad (2)$$

where θ is the scattering angle; $I(\theta, \lambda, t)$ the output voltage in the aureole; $\tau_a(\lambda, t)$ the aerosol optical depth; and $P(\cos\theta)$ the columnar scattering phase function. The second equality in Eq. (2) is derived from single scattering consideration in solving the radiative transfer equation (Green et al. 1971). Eq. (2) clearly indicates that the relative aureole must remain constant with m or time if the aerosol optical depth remains unchanged. Temporal variation of the ratio will be indicative of aerosol optical instability.

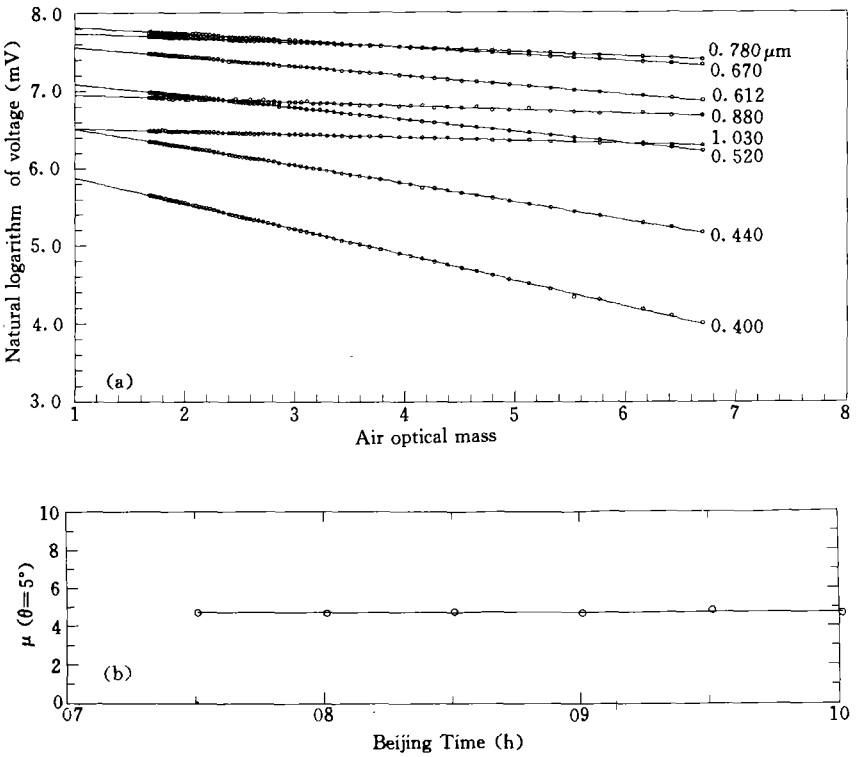

Fig. 1. On an optically stable day (Nov. 22, 1993) at Mt. Huangshan: (a) Langley plots for eight wavelengths, and (b) temproal variation of relative aureole for 5° scattering angle and 0.52 μm wavelength.

As an example, Figures 1 and 2 represent Langley plots for all eight wavelengths and corresponding relative aureoles for 5° scattering angle and 0.52 μm wavelength on the optically stable and unstable day, respectively. For each wavelength, sufficient linear Langley plots were obtained on the two days. All mean absolute deviations of observed Langley plots from the corresponding regression lines were smaller than 0.005 and correlation coefficients were higher than 99.0%. However, the relative aureoles for the two days were quite different. The relative aureole remained almost constant during the whole morning of Nov. 22, 1993. The slop of linear-fitting through the data points was only +0.0008. In contrast, during the afternoon of Nov. 24, 1993, the relative aureole gradually increased, whose slop was +0.13, indicating a steady increase of aerosol loading above the measurement site. Figure 3 gives the time pattern of aerosol optical depth at 0.52 μm wavelength in the afternoon of Nov. 24, 1993 calculated from the calibrated value. It is apparent that the aerosol optical depth is gradually increased in a form of τ_a (0.52 μm, t) = 0.0047t − 0.0366, whose correlation coefficient is 95.28%, or in a form of τ_a (0.52 μm, m) = −0.0328/m+0.0482, whose correlation coefficient is 95.17%.

The example clearly shows that it is difficult to assess the quality of the Langley plots based on the linearity of the regression data alone. The intercept of regression line for Langley plots with large relative aureole variation has to be rejected even though the

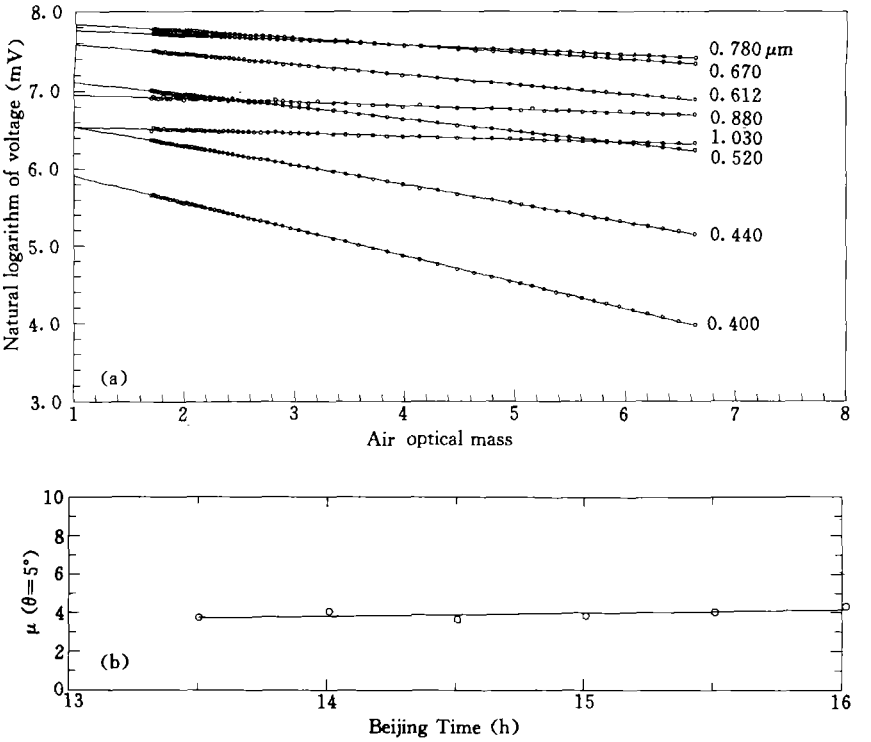

Fig. 2. As in Fig. 1, but on an optically unstable day, Nov. 24, 1993.

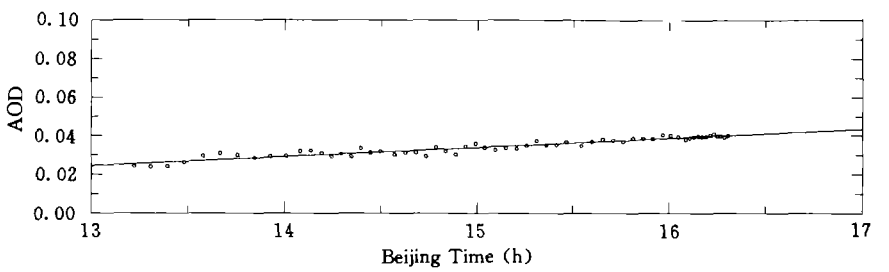

Fig. 3. Time evolution of aerosol optical depth (AOD) at 0.52 μm wavelength on Nov. 24, 1993, at Mt. Huangshan.

Langley plots appear sufficient linear. The true intercept chosen as the calibrated value should be based on both sufficient linear Langley plots and a comparatively small variation of the relative aureole.

The sun-photometer was calibrated successfully on two mornings and one afternoon, each of which was judged to have relatively stable aerosol content by using the above-mentioned method. According to the error analysis of the calibrated values at Mt. Huangshan (Zhou et al. 1994), the calibration errors for all eight wavelengths were less than 1%.

IV. DATA PROCESSING AND ERROR ANALYSIS

When the calibrated sun-photometer is used to take solar spectral extinction

measurements, an instantaneous atmospheric optical depth can be determined from its output voltage $V(\lambda, t)$ at time t and the calibrated value $V_0(\lambda)$ by

$$\tau(\lambda, t) = \frac{1}{m(t)} \ln \frac{RV_0(\lambda)}{V(\lambda, t)}. \tag{3}$$

The instantaneous aerosol optical depth is obtained by subtracting the contributions due to Rayleigh scattering (Teillet 1990), ozone Chappuis absorption (Show 1979; Van Heuklon 1979) and nitrogen dioxide absorption (Tomasi 1985) from the instantaneous atmospheric optical depth:

$$\tau_a(\lambda, t) = \tau(\lambda, t) - \tau_R(\lambda) - \tau_{O_3}(\lambda) - \tau_{NO_2}(\lambda). \tag{4}$$

Its mean value over the day can be written as

$$\tau_a(\lambda) = \frac{\sum_{n=1}^{N} \tau_{a_n}(\lambda, t)}{N}, \tag{5}$$

where N is the number of measurement during observational period.

Relative errors made in evaluating the instantaneous aerosol optical depths can be estimated through the equation:

$$\rho(\lambda, t) = \pm \left[\frac{1}{m(t)} \left|\frac{\Delta V_0(\lambda)}{V_0(\lambda)}\right| + \frac{1}{m(t)} \left|\frac{\Delta V(\lambda, t)}{V(\lambda, t)}\right| + \Delta\tau_R(\lambda) + \Delta\tau_{O_3}(\lambda) + \Delta\tau_{NO_2}(\lambda)\right] / \tau_a(\lambda, t). \tag{6}$$

This expression has taken into account uncertainties in calibration values, instantaneous output voltages, Rayleigh, ozone and nitrogen dioxide optical depths, respectively. As mentioned in above sections, the measurement and calibration errors are 1% respectively. Uncertainties for Rayleigh, ozone and nitrogen dioxide optical depths are 1%, 15% and 30%, respectively (Russell et al. 1979; 1993). Thus, the overall relative errors for instantaneous aerosol optical depths are estimated to be about 10%. As an example, for 0.52 μm wavelength, the aerosol, Rayleigh, ozone and nitrogen dioxide optical depths are typically 0.4, 0.1175, 0.0168 and 0.0203, respectively. Thus, the relative error for instantaneous aerosol optical depths at 0.52 μm wavelength is about 6% when atmospheric optical mass is 2.

V. TEMPORAL VARIATIONS OF AEROSOL OPTICAL DEPTHS AND ANGSTROM TURBIDITY PARAMETERS

1. *Within-Year Variation in Aerosol Optical Depths*

Figure 4 shows the variation of monthly average aerosol optical depths for the eight wavelengths during the period September of 1993 through September of 1994. The wavelengths corresponding to the eight curves from bottom to top are 1.03, 0.88, 0.78, 0.67, 0.612, 0.52, 0.44 and 0.40 μm, respectively. It is apparent that the aerosol extinction decreased well with increasing of wavelength for all months. The aerosol optical depths generally were confined in the range between 0.1 and 0.8, that is nearly ten times that at Tucson, Arizona (King et al. 1980), indicating high aerosol loading over Hefei. The aerosol optical depths were also found to increase progressively from September 1993 to April 1994, then decrease until July 1994, subsequently increase again. They appeared to

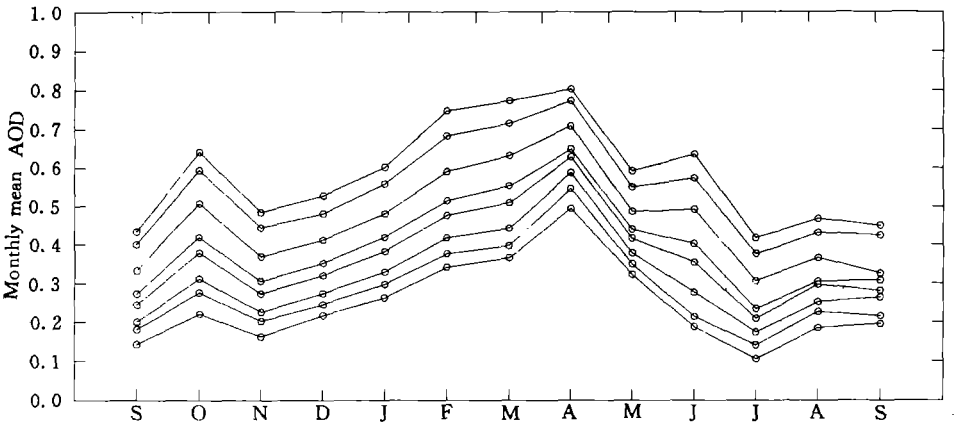

Fig. 4. Monthly average values of aerosol optical depths (AOD). The eight curves from bottom to top correspond to aerosol optical depths of 1.03, 0.88, 0.78, 0.67, 0.612, 0.52, 0.44 and 0.40 μm wavelength, respectively.

be a distinct seasonal variation, having larger values in spring, smaller in summer, and intermediate in autumn and winter.

The characteristics of seasonal differences of aerosol optical depths are closely related to the seasonal variation of the synoptic weather pattern occurring around Hefei. Hefei is located in the southeast part of China. It is situated in boundaries of subtropical and temperate zones. During the autumn and winter months a north or northwesterly current system with dry, cold and rather clean air mass usually prevails over Hefei. The local aerosol particles are diluted. In the spring, the cold, dry air mass interfaces with warm, wet air mass carried by southwest current. Sometimes, both currents match each other in strength, forming stagnant air flow. This stagnant air flow contributes to the accumulation of local aerosol particles in the mixed layer. The damp haze layer is thick, steady and the sky appears gray-white during this time period. On the other hand, yellow sand particles uplifted in the northern China are usually transported to Hefei area by front activities. The dust storm event also contributes significantly to the atmospheric turbidity. During the summer months, the Pacific high pressure system with clean air dominates the weather pattern. At the same time, thunderstorms occur frequently in the early afternoon. The heavy shower removes the local aerosol particles efficiently. After thunderstorm, the air becomes very fresh and clean, the sky appears blue and the transparency of atmosphere becomes high. These factors cause the summer minimum in aerosol optical depths over Hefei.

2. *Within-Year Variation of Angstrom Turbidity Parameters*

Spectral dependence of the aerosol optical depths follows the Angstrom formula very well throughout the whole spectral range from 0.4 to 1.0 μm wavelength:

$$\tau_a(\lambda) = \beta\lambda^{-\alpha}, \tag{7}$$

where $\tau_a(\lambda)$ is aerosol optical depth; λ wavelength (μm); β Angstrom turbidity coefficient; and α Angstrom wavelength exponent. The turbidity coefficient β is a measure of

the quantity of aerosol particles and gives the best-fit value of the aerosol optical depth at 1 μm wavelength. The wavelength exponent α is closely related to aerosol size distribution. It will decrease as the weight of large aerosol particles on the spectral aerosol optical depths increases. Therefore, the different values of α can be interpreted as the variable contribution of the different models to size distribution of aerosol particles. For Junge-type aerosol size distribution it has a relation $u=\alpha+2$, where u is Junge exponent. Values of α close to zero are associated with high loads of large aerosol particles, whereas value of 2 indicates that the aerosol particle content is mostly composed of Aiken nuclei. The Angstrom turbidity parameters fully describe the aerosol particle extinction characteristics along the vertical path.

From data observed from our sun-photometer measurements the Angstrom turbidity parameters have been obtained by means of a log-log regression of the measured aerosol optical depths versus wavelengths. It was found that the correlation coefficients for the regressions were larger than 99.0% on most days of the one year period. This indicates that the Angstrom formula indeed reflects spectral characteristics of the aerosol optical depths in real atmospheric conditions.

Figure 5 shows the variations of monthly average Angstrom turbidity parameters during this one year period. The open circles represent the Angstrom wavelength exponents and the open triangles give the Angstrom turbidity coefficients. It is apparent that the turbidity coefficients were generally observed from 0.5 for spring hazy days to 0.1 for summer clean days. On July 6, 1994, the turbidity coefficient dropped to 0.04, the minimum value in this one year period. The minimum turbidity coefficient is of special significance since it tends to represent the least polluted situation, hence the value can be considered as the background level of atmospheric aerosol over Hefei. On the other hand, the values of wavelength exponents ranged from 0.5 to 1.4, corresponding to the Junge exponent between 2.5 and 3.4. The overall mean value is 0.95 with a standard deviation of 0.27.

In Fig. 6, the wavelength exponents are plotted as a function of the turbidity coefficients. This figure shows the above-mentioned results more clearly. It can also be seen that the wavelength exponents generally decreased with the increase of turbidity

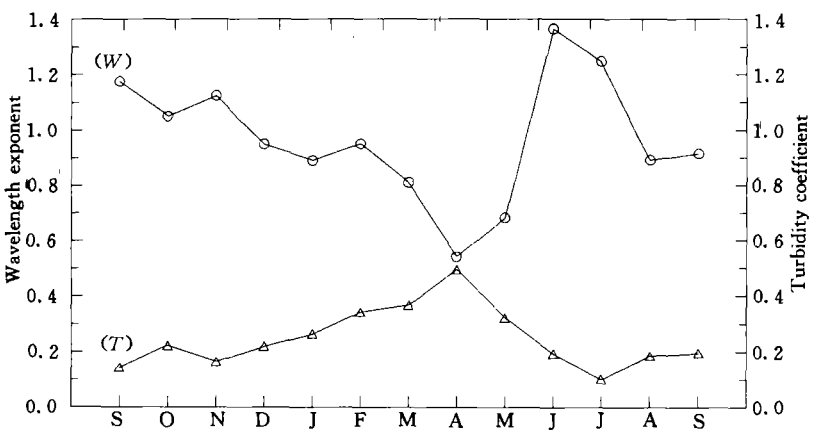

Fig. 5. Monthly average values of Angstrom turbidity coefficients (T) and wavelength exponents (W).

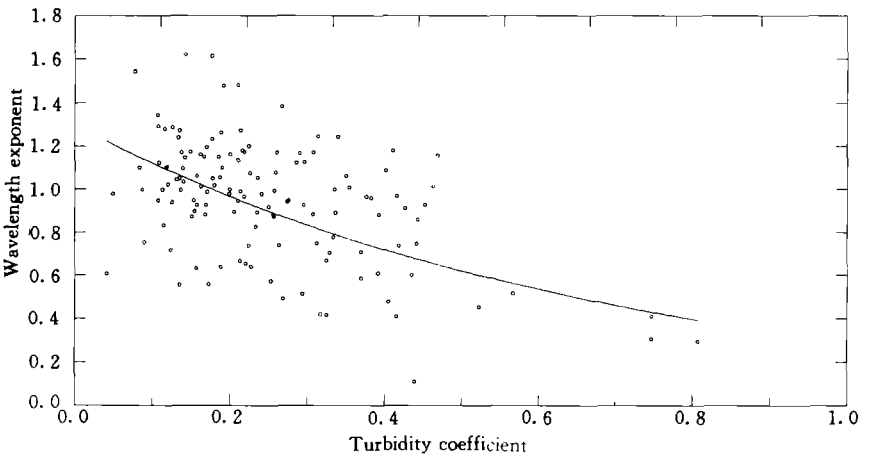

Fig. 6. Angstrom wavelength exponent as a function of turbidity coefficient. The exponential regression curve of best fit through these data is expressed by $\alpha=1.30\exp(-1.48\beta)$.

coefficients. An exponential regression curve of best fit through these data is expressed as $\alpha=1.30\exp(-1.48\beta)$. This negative correlation between wavelength exponent and turbidity coefficient is also found by many investigators, e. g. Kaufman et al. (1983), Mohamed et al. (1992), Prodl et al. (1984), and Tanaka et al. (1989). This means that the atmospheric turbidity generally increases with the increase of concentration of large aerosol particles.

3. *Diurnal Evolution of the Aerosol Optical Depth*

Figure 7 displays diurnal variations in aerosol optical depth at 0.52 μm wavelength during the selected afternoon. As can be seen, the diurnal evolution behavior of the aerosol optical depth appeared very variable. The aerosol optical depth could gradually increase (a), decrease (b), or even could remain almost constant (c) (slops of linear-fitting through the data points were less than ± 0.005) during the afternoon hours. Similar evolutions of aerosol optical depths were observed during the morning hours. We believe that the results in Fig. 7 represent a real atmospheric effect. The reason for this is that during the days with constant aerosol optical depths, relative differences between the intercepts determined by linear regression of Langley plots and the calibrated values of $R\ln(V_0(\lambda))$ corrected for sun-earthdistance were less than 0.01 for all wavelengths. Meanwhile, horizontal visibilities obtained from hourly reports at the nearby Hefei airport and aerosol concentration measured by our ground-based optical particle counter also generally appeared to be constant values during the same period of time.

The mechanisms which cause the within-day variation of aerosol optical depth are rather complecated. This variation is closely related to production, transport, dispersion and removal of aerosol particles in the sunlight path. Many time-dependent factors, including synoptic weather system, the type of air mass and local meteorological elements, such as relative humidity, temperature, precipitable water, wind speed and direction, might be involved in the diurnal variation process. Peterson et al. (1981) have generally given the reason for diurnal circle of aerosol optical depth, such as maximum daytime

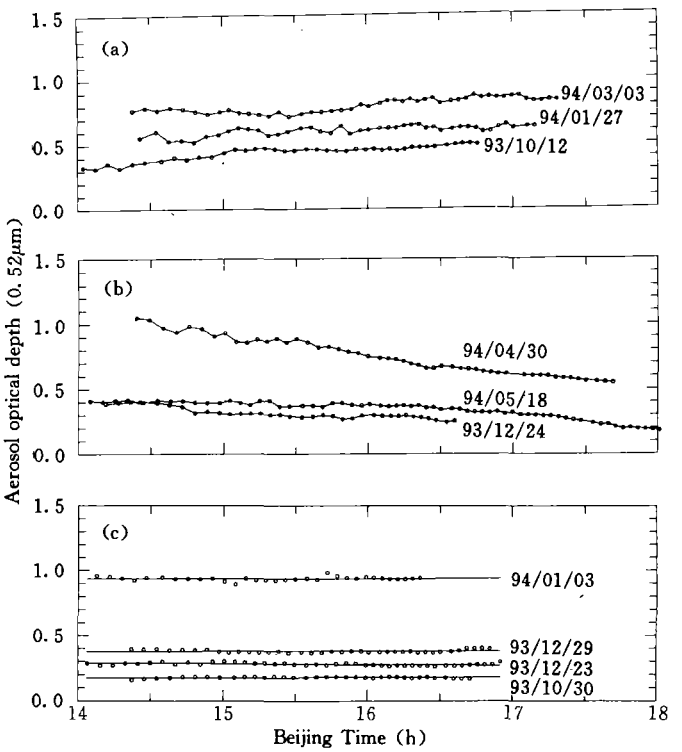

Fig. 7. Time evolutions of aerosol optical depth at 0.52 μm wavelength during the afternoon hours.

anthropogenic activities, daily circle of solar radiation intensity and diurnal variation of mixing height and temperature. However, although all these factors probably have some impact on within-day variation of aerosol optical depth, his available information was not sufficient to rank them. Liu et al. (1990) have found that aerosol optical depth increases with the destabilization of the boundary layer through analyzing the relationship between aerosol optical depth and the Turner stability factor.

As mentioned above, the aerosol optical depth characterizes the extinction of aerosol contained in the whole air column. Thus, the aerosol particles within mixed layer are responsible for greatest part of the column extinction. Therefore, the diurnal evolution of aerosol optical depth is mainly determined by the feature of aerosol particles in the mixed layer.

When the surface of earth is heated by the sun during the daytime, the produced thermal convection carries aerosol particle aloft. The vertical convective aerosol plume structure first appears an hour or two after sunrise, thickens gradually and reaches a depth from a few hundred to a few thousand meters by early afternoon (Zhou et al. 1988). Then, the solar radiation intensity decreases and thermal convection becomes weaker. The aerosol particles from elevated sources tend to settle downwards and fall to the surface. The depth of the mixed layer decreases gradually. This can probably explain one of diurnal circles of aerosol optical depth, i.e., an increase during the morning and a decrease in the afternoon.

It was found that constant aerosol optical depth had a close relation with frontal

passage, or duststorm event. When these happened, strong west or northwest winds with 6—7 m/s usually lasted for one or two days. On the following half or one day after the frontal passage, the aerosol particles were mixed very well, remaining stratus and horizontal uniform. The vertical mass loading of aerosol particles was kept nearly constant.

From this it follows that the diurnal evolution of aerosol optical depth may be determined by a combination of many complex processes. Single factorial analysis or simple description can be hardly made of it. So far, not all the mechanisms for diurnal variation of aerosol optical depth are clear. Therefore, further understanding of these mechanisms requires a great deal of observational studies, such as measurements of the above mentioned time-dependent factors by instrumented radiosonde, airplane, or lidar simultaneously with the sun-photometer measurements.

VI. SPECTRAL DEPENDENCE OF AEROSOL OPTICAL DEPTHS AND CORRESPONDING SIZE DISTRIBUTIONS

The equation which relates aerosol optical depth to columnar aerosol size distribution can be written as

$$\tau_a(\lambda) = \int_0^\infty \pi r^2 Q_{ext}(r, \lambda, m^*) n_c(r) \mathrm{d}r, \tag{8}$$

where $n_c(r)$ $(=\mathrm{d}N_c(r)/\mathrm{d}r)$ is columnar aerosol size distribution; $Q_{ext}(r, \lambda, m^*)$ extinction efficiency factor of aerosol with radius r and complex refractive index m^*. It is the ratio of the extinction cross section to the geometric cross section for a spherical aerosol particle and can be evaluated through Mie scattering theory (Dave 1968). The linearly-constrained inversion method (King et al. 1978) is used to retrieve the columnar aerosol size distribution from the spectral aerosol optical depths. In the inversion calculation, the complex refractive index of aerosol particles was preset to $1.50-0.01i$ (Tanaka et al. 1989). The radius range of retrieval was from 0.1 to 1.2 μm and divided into 8 intervals. Error analysis shows that the errors of inverted aerosol size distribution $\Delta n_c(r)/n_c(r)$ depend on the atmospheric turbidity. Under haze and moderate turbidity, the errors for all eight aerosol sizes were less than 10% and mean relative error was about 6%. Comparing aerosol optical depths calculated from the retrieved size distributions with the measured ones shows that their relative errors were less than 3%. On clear days, however, the errors of retrieved size distributions were as large as 20% for the two sizes between 0.9 and 1.2 μm. For the rest six sizes the errors were still 10%. In this case, the mean relative errors were about 15% and the relative errors between the calculated and measured aerosol optical depths were about 5%.

Three representative days, April 30, 1994 (haze day), September 25, 1993 (moderate turbidity) and July 6, 1994 (background), are selected to investigate the spectral characteristics of aerosol optical depths and aerosol size distributions. The wavelength dependence of aerosol optical depths and corresponding columnar size distributions for the three days are shown in Figs. 8a and 8b, respectively. For comparison, the results of background aerosols at Mt. Huangshan on November 28, 1990 are also given in the figure.

As can be seen from Fig. 8a, the spectral aerosol optical depths on the hazy day at Hefei were almost 1.5—2 orders of magnitude as large as that at Mt. Huangshan. Even on

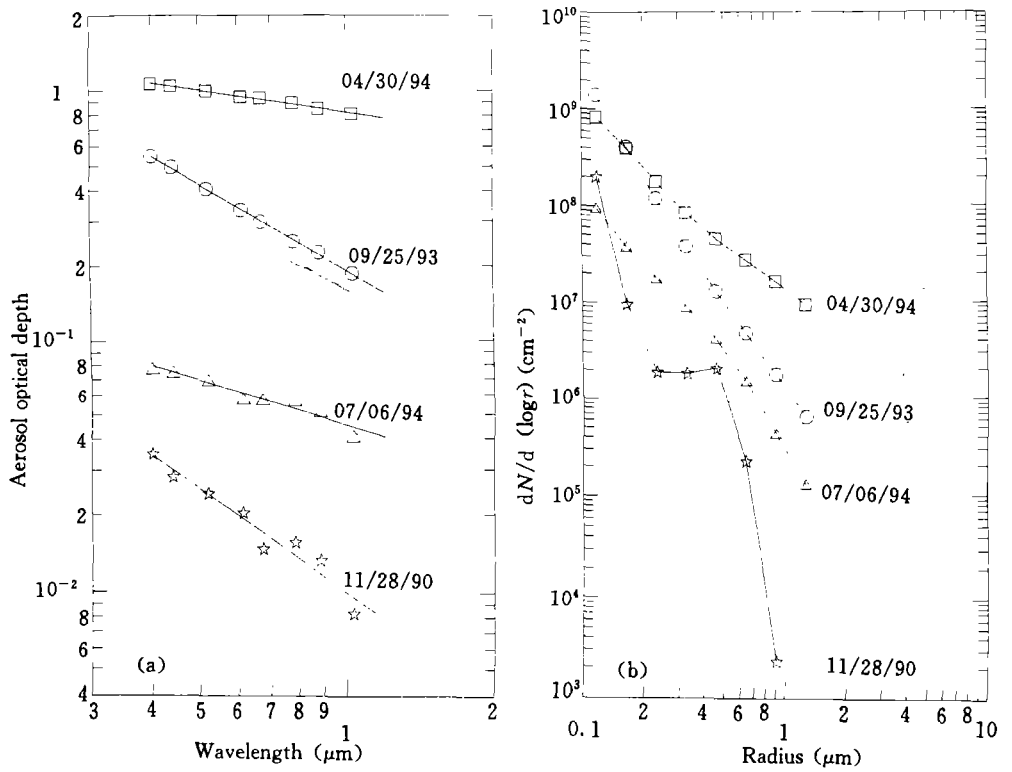

Fig. 8. (a) Wavelength dependence of aerosol optical depths and (b) corresponding aerosol size distributions. The symbol of five-pointed star stands for the results observed at Mt. Huangshan on November 28, 1990.

the moderate turbidity days, there were still nearly ten time differences between them. On the other hand, from Fig. 8b it is evident that the corresponding number densities of aerosols around 1 μm radius exhibited great differences, but, for small particles around 0.1 μm radius, the differences were not noticeable. It seems that the aerosol particles with radii around 1 μm are greatly responsible for the aerosol extinction in the visible and near infrared spectral range.

From the figure, it can also be seen that for April 30, 1994 and September 25, 1993, the log-log regression of the measured aerosol optical depths versus wavelengths appeared to be sufficient linearity with correlation coefficients of 99.95% and 99.15%, respectively. This indicates the spectral characteristics of aerosol optical depths can be best expressed by the Angstrom formula under hazy and moderate turbidity atmospheric conditions. At the same time, the corresponding column size distributions exhibited Junge type of size distributions. Most of our observational data during this one year period present similar feature like this. Curcio (1961) also found that the higher attenuation data cases tended to be dominated by Junge-type size distributions. That is in essential agreement with the results presented here.

On occasions when the aerosol optical depths were very small, such as July 6, 1994 at Hefei and November 28, 1990 at Mt. Huangshan, the correction coefficients between aerosol optical depths and the wavelengths were 96.90% and 97.24%, respectively, and

the retrieved aerosol size distributions could be best described as consisting of two types of size distributions. This two-component size distribution is consistent with the production mechanisms of atmospheric aerosols. Aerosol particles in the accumulation range with radii from about 0. 01 to 0. 5 μm typically arise from condensation of low volatility vapor and from coagulation of smaller particles in the nuclei range. Particles in the coarse range having radii larger than about 1. 0 μm are usually produced by mechanical processes such as grinding, wind or erosion. It is not surprising that the two production mechanisms are not very effective in the 0. 5—1. 0 μm range, and thus separation of the two regions might sometimes be observed.

VII. CONCLUSIONS

The following conclusions may be drawn from the solar spectral extinction measurements at Hefei during the one year period:

(1) During the Langley calibration period, measurements of the relative solar aureole were shown to be a very effective method of monitoring temporal stability of aerosol content. The true intercepts chosen as the calibrated values should be based on both the sufficient linear Langley plots and a comparatively small temporal variation of the relative aureole.

(2) The monthly average values of aerosol optical depths for all eight wavelengths in the visible and near infrared spectral range generally were confined in the range 0. 1 and 0. 8. They had distinct seasonal variation, with larger values in the spring, smaller in the summer and intermediate during the autumn and winter months. This seasonal variation of aerosol optical depths is closely related to the seasonal variation of the synoptic weather pattern occurring around Hefei.

(3) The monthly average values of Angstrom turbidity coefficients were generally observed from 0. 5 for hazy day to 0. 1 for rather clean day. The background value was found around 0. 04. The monthly average values of Angstrom wavelength exponents ranged from 0. 5 to 1. 4. Its overall mean value was 0. 95 with a standard deviation of 0. 27. The negative correlation existing between the two Angstrom parameters suggests that the atmospheric turbidity increases with an increase of concentration of larger aerosol particles.

(4) The diurnal evolution of aerosol optical depth over Hefei appeared very variable. It could gradually increase, decrease, or even could remain almost constant. The mechanisms causing the within-day variation of aerosol optical depths are rather compli ated. This variation is closely related to production, transport, dispersion and removal of aerosol particles in the sunlight path. Single factorial analysis or simple description can be hardly made of it. Fully understanding of the mechanisms of this variation requires a great deal of theoretical and observational work.

(5) On most days, the atmosphere over Hefei appeared to be in hazy or moderate turbidity. In these cases, the spectral characteristics of aerosol optical depths could be best expressed by the Angstrom formula, and the corresponding aerosol size distributions exhibited Junge type of size distributions. Under very clean air conditions, a two-slop type of aerosol size distribution could be retrieved.

REFERENCES

Curcio, J. A. (1961). Evaluation of atmospheric aerosol particle size distribution from scattering measurements in the visible and infrared. *J. Opt. Soc. Amer.*, **51**: 548—551.

d'Almeida, G. A. et al. (1983). New sun-photometer for network operation. *Appl. Opt.*, **22**: 3796—3801.

Dave, J. V. (1968). Subroutines for computing the parameters of the electromagnic radiation scattering by a sphere. *IBM Report*.

Flowers, E. C. et al. (1969). Atmospheric turbidity over the United States, 1961—1966. *J. Appl. Meteor.*, **8**: 955—962.

Green, A. E. S. et al. (1971). Interpretation of the sun's aureole based on atmospheric aerosol models. *Appl. Opt.*, **10**: 1263—1270.

Herman, B. M. et al. (1981). Alternate approach to analysis of solar photometer data. *Appl. Opt.*, **20**: 2925—2928.

Kaufman, Y. J. et al. (1983). Light extinction by aerosol during summer air pollution. *J. Climate Appl. Meteor.*, **22**: 1694—1706.

King, M. D. et al. (1978). Aerosol size distributions obtained by inversion of spectral optical depth measurements. *J. Atmos. Sci.*, **35**: 2153—2167.

King, M. D. et al. (1980). Spectral variation of optical depth at Tucson, Arizona between August 1975 and December 1977. *J. Appl. Meteor.*, **19**: 723—732.

Li, J. and Mao, J. (1990). Properties of atmospheric aerosols inverted from optical remote sensing. *Atmos. Environ.*, **24A**: 2517—2522.

Liu, C. M. and Feng, T. S. (1990). Atmospheric turbidity over Taiwan. *Atmos. Environ.*, **24A**: 1303—1312.

Mao, J. and Luan, S. (1985). Derivation of scattering phase function from clear sky brightness distribution. *Adv. Atmos. Sci.*, **2**: 129—131.

Mohamed, A. B. and Frangi, J. P. (1986). Results from ground-based monitoring of spectral aerosol optical thickness and horizontal extinction: some specific characteristics of dusty Sahelian atmospheres. *Geophy. Res. Lett.*, **25**: 1807—1815.

Mohamed, A. B. et al. (1992). Spatial and temporal variations of atmospheric turbidity and related parameters in Niger. *J. Appl. Meteor.*, **31**: 1286—1294.

O'Neill, N. T. and Miller, J. R. (1984). Combined solar aureole and solar bean extinction measurements, 1: calibration considerations. *Appl. Opt.*, **23**: 3691—3696.

Peterson, J. T. et al. (1981). Atmospheric turbidity over central north Carolina. *J. Appl. Meteor.*, **20**: 229—241.

Pink, R. T. et al. (1994). Characteristic aerosol optical depths during the Harmattan season on sub-Sahara Africa. *Geophy. Res. Lett.*, **21**: 685—688.

Prodi, F. et al. (1984). Measurements of atmospheric turbidity from a network of sun-photometers in Italy during ALPEX. *J. Aerosol Sci.*, **15**: 595—613.

Qiu Jinhuan et al. (1986). Simultaneous determination of aerosol size distribution and refractive index and furnace albedo from radiance—Part II: Application. *Adv. Atmos. Sci.*, **3**: 341—348.

Qiu Jinhuan (1988). The remote sensing of the properties of atmospheric aerosols in Beijing city. *Acta Met. Sinica*, **46**: 49—58 (in Chinese).

Russell, P. B. and Show, G. E. (1975). Comments on "the precision and accuracy of Volz sunphotometry", *J. Appl. Meteor.*, **14**: 1206—1209.

Russell, P. B. et al. (1979). Aerosol-induced albedo change: Measurement and modeling of an incident. *J. Atmos. Sci.*, **36**: 1587—1608.

Russell, P. B. et al. (1993). Pinatubo and pre-Pinatubo optical depth spectra: Mauna Loa

measurements, comparisons, inferred particle size distributions, radiative effects, and relationship to lidar data. *J. Geophy. Res.*, **98**: 22969—22985.

Shaw, G. E. (1979). Atmospheric ozone: Determination by Chappius-band absorption. *J. Appl. Meteor.*, **18**: 1335—1339.

Tanaka, M. et al. (1989). Aerosol optical characteristics in the yellow sand events observed in May, 1982 at Nagasaki—Part I: Observations. *J. Meteor. Soc. Japan.*, **67**: 267—278.

Tanre, D. et al. (1988). Radiative properties of desert aerosol by optical ground-based measurements at solar wavelengths. *J. Geophy. Res.*, **93**: 14223—14231.

Teillet, P. M. (1981). Rayleigh optical depth comparisons from various sources. *Appl. Opt.*, **29**: 2925—2927.

Tomasi, C. et al. (1985). Multiwavelength sun-photometer calibration corrected on the basis of spectral features characterizing particulate extinction and nitrogen dioxide absorption. *Appl. Opt.*, **24**: 2962—2970.

Van Heuklon, T. K. (1979). Estimating atmospheric ozone for solar radiation models. *Solar Energy*, **22**: 63—68.

Zhou Jun et al. (1987). Atmospheric aerosol optical depths and size distributions at Hefei and Huangshan mountain. Atmospheric Radiation: Progress and Prospects. Science Press. pp. 608—618.

Zhou Jun et al. (1988). Infrared lidar measurements of crustal aerosol mixing in the troposphere. *Appl. Opt.*, **27**: 2639—2640.

Zhou Jun et al. (1994). Sun-photometer calibration and its application. *Acta Met. Sinica*, **8**: 230—237.